

Electrochemical study on magnesium anodes in NaCl and CaSO₄–Mg(OH)₂ aqueous solutions

Fidel Guadarrama-Muñoz^a, Juan Mendoza-Flores^a, Ruben Duran-Romero^a, J. Genesca^{b,*}

^a Mexican Petroleum Institute, Exploration and Production Corrosion, Eje Central L. Cardenas, 152, Mexico 07730 DF, Mexico

^b Corrosion Laboratory, Department of Metallurgical Engineering, Faculty of Chemistry, UNAM, 04510 Mexico DF, Mexico

Received 23 June 2004; received in revised form 29 November 2004; accepted 25 February 2005

Available online 1 September 2005

Abstract

The anodic dissolution behavior of three samples of magnesium anodes, with different electrochemical efficiency, was studied in two test aqueous solutions: 3% NaCl and saturated CaSO₄·2H₂O–Mg(OH)₂. Polarization curves and electrochemical impedance spectroscopy (EIS) were used. It was found that activation processes takes place at the metal–electrolyte interface. These processes can be represented by two parallel electric equivalent circuits, arranged in series, and in series with the resistance of the solution. It is proposed that the physical meaning of the two parallel circuits can be associated to a charge transfer process and to the presence of a layer of corrosion products on the surface of the metal.

© 2005 Elsevier Ltd. All rights reserved.

Keywords: Cathodic protection; Current efficiency; EIS; Magnesium anodes

1. Introduction

At the time, there are two laboratory tests methods for the evaluation of magnesium anodes used in the cathodic protection industry of Mexico. These methods are based on the mass loss of magnesium test samples, immersed in a defined test environment, during a determined period of time and at a constant anodic current density. Both methods intend to provide a way of comparing the performance of different anode alloys in a controlled environment. One method is the ASTM G-97-97, “standard tests method for laboratory evaluation of magnesium sacrificial anode test specimens for underground applications” [1]. The second method is described by the Mexican standard NMX–K–109–1977, “magnesium anodes used in cathodic protection” [2].

The efficiency of Mg anodes usually is determined using the ASTM G97-97 [1] test method, which involves cutting and machining five 12.7 by 152 mm specimens from an anode

casting. The specimens are placed in separate containers with a calcium sulfate, CaSO₄/magnesium hydroxide, Mg(OH)₂ electrolyte, connected in series with coulometers and powered at a constant current density of 0.039 mA cm⁻² for 14 days. The weight loss during the test period is compared to the theoretical weight loss calculated based on coulometer measurements. The Mexican test method indicates a test environment made of artificial sea water, a testing current density of 1.25 mA cm⁻² and a testing time between 96 and 120 h. Both testing methods are in fact galvanostatic tests, in which a known direct current is passed through test cells connected in series in order to determine efficiency of sacrificial anode materials.

To a considerable extent anode efficiencies have been reported only for the 36 (0.039 mA cm⁻²) and 72 mA ft⁻² current densities since these correspond most closely to the current densities encountered in actual underground service [3]. The Mexican NOM K 109–1977 is a more severe test than its ASTM counterpart and anode current density, 1.25 mA cm⁻² exceeds normal underground service, but with short testing period.

* Corresponding author. Fax: +52 55 56225228.

E-mail address: genesca@servidor.unam.mx (J. Genesca).

Table 1
Relevant measured parameters for M1, M2 and M3 magnesium anodes samples

| Sample | Measured A h lb ⁻¹ | | Efficiency (%) | |
|----------------------------------|-------------------------------|---------------|----------------|---------------|
| | ASTM G-97-97 | NMX K109-1977 | ASTM G-97-97 | NMX K109-1977 |
| M1 | 547.32 | 564.4 | 54.7 | 56.5 |
| M2 | 360.07 | 387.2 | 36 | 38.7 |
| M3 | 130.51 | 172.86 | 13 | 17.28 |
| Reference value (NMX-K-109-1977) | N/A | 500 (minimum) | N/A | 50 (minimum) |

The variation in electrochemical efficiency among both tests is quite significant. Over the years, these differences have caused controversy on the way magnesium anodes should be evaluated in laboratory. It is interesting to note that the open circuit potential generally becomes increasingly electronegative as the efficiency increases. The reason for the efficiency variation and the relatively low efficiency compared to the theoretical value is not well understood, probably because of the large number of factors that can affect the efficiency. Few electrochemical data is available in order to support the decision on which test method should be used. This work explores both testing methods in order to provide valuable electrochemical information that can help to understand the different current (electrochemical) efficiency values obtained under these two standards.

2. Experimental procedure

All experiments were carried out in a three electrode 1 L glass cell. Two sintered graphite rods were used as counter electrodes (CE). The reference electrode (RE) was a saturated calomel electrode (SCE). In order to reduce IR drop effects in all measurements a Lugging capillary was used. A Mg alloy sample, encapsulated in phenolic resin, was used as working electrode (WE). Polarization curves were recorded using an ACM GILL AC potentiostat controlled by a personal computer. Electrochemical impedance measurements were carried out using a SOLARTRON 1280B potentiostat–galvanostat, controlled by a personal computer.

2.1. Working electrodes (electrochemical efficiency)

Three magnesium anode samples with different electrochemical efficiencies (see Table 1) were tested. These samples were identified as M1, M2 and M3. The electrochemical efficiency of each sample was previously measured by both ASTM and NMX methods. Cylindrical rods were machined from M1, M2 and M3 magnesium anodes in order to construct the working electrodes. All working electrodes were encapsulated in phenolic resin, leaving only a circular area exposed of 1 cm². Before each experiment, the WE was wet polished with 600 SiC paper, rinsed with deionized water and degreased with acetone.

Magnesium anode samples were provided by different manufacturers. Table 2 shows the chemical (elemental) com-

position of each sample, obtained by atomic absorption. Magnesium fines produced during cutting and machining operations were dissolved in an aqueous solution of HCl and then analyzed by atomic absorption, AA.

2.2. Testing solutions

Two testing aqueous solutions were used in the experimentation. One solution was 3% NaCl. This solution was selected in order to have an environment of simple chemical composition that allows the understanding of the electrochemical process taking place on the surface of the magnesium alloys. The second testing solution had the chemical composition indicated by the ASTM G97 procedure [1], 5 g of reagent grade CaSO₄·5H₂O, 0.1 g of reagent grade Mg(OH)₂ to 1000 mL or reagent grade water. All experiments were carried out at 20 °C and at the atmospheric pressure of Mexico City (0.7 bar). All testing solutions were prepared with Aldrich reagent grade chemicals.

2.3. Open circuit potential (E_{oc}) versus time

The E_{oc} of each sample was measured against a saturated calomel electrode (SCE). The E_{oc} values were recorded each second for a period of 20 h approximately, for each of alloy sample immersed in each testing environment. The measured values are shown in Table 3. In order to obtain a representative value of E_{oc} for each condition, all the measured values of E_{oc} were averaged, after 2.5 h of immersion time.

Table 2
Main chemical elements determined by atomic absorption in M1, M2 and M3 samples of magnesium alloys

| Chemical composition (wt.%) | Sample | | | |
|-----------------------------|-----------------------|-------|-------|-------|
| | Reference (ASTM B843) | M1 | M2 | M3 |
| Al | 0.01 max | <0.01 | 0.01 | 7.2 |
| Cu | 0.02 max | 0.001 | 0.001 | 0.13 |
| Fe | 0.03 max | 0.01 | 0.002 | 0.006 |
| Mn | 0.5–1.3 | 0.07 | 0.75 | 0.18 |
| Ni | 0.001 max | 0.001 | 0.001 | 0.004 |
| Others | 0.3 max | | | |
| Zn | | 0.003 | 0.01 | 3.92 |
| Mg | Balance (98.33) | 99.1 | 94.94 | 85.94 |
| Total | | 99.2 | 95.71 | 97.35 |

Table 3

Averaged open circuit potential (E_{oc}), for each sample of magnesium anode, in the two test solutions

| Sample | E_{oc} mV vs. SCE (averaged after 2.5 h of exposure time) | |
|--------|---|------------------------|
| | 3% NaCl solution | ASTM G97 test solution |
| M1 | -1698.58 | -1535.32 |
| M2 | -1600.66 | -1571.89 |
| M3 | -1535.32 | -1571.89 |

Averages calculated after 2.5 h initials for 20 h of immersion time.

2.4. Polarization curves

Polarization curves were carried out, in each testing solution, after 6 h of exposure time. This period of time assures that a near steady-state conditions of the E_{oc} ($\Delta E \leq 10$ mV for 60 min) are reached. All polarization curves were recorded potentiodynamically with a sweep rate of 10 mV min^{-1} . A potential range of ± 300 mV, referred to E_{oc} , was selected.

2.5. Electrochemical impedance spectroscopy (EIS)

Potentiostatic EIS measurements were carried out in a frequency range of 0.01–10,000 Hz and an amplitude of 10 mV (referred to E_{oc}) and eight data points per decade of frequency were recorded. Each EIS experiment was performed after what the E_{oc} reached the steady-state. Only for the M1 sample immersed in the 3% NaCl solution, EIS measurements were carried out at three fixed anodic potentials, away from the steady-state E_{oc} . These three anodic potentials were: 85, 145 and 200 mV (referred to E_{oc}). It can also be observed that sample M1 is the only one that fulfills the specified requirement of $564.4 \text{ A h lb}^{-1}$, indicated in the NMX standard method [2]. In this standard a value of 500 A h lb^{-1} need to be reached as a minimum, which corresponds to an electrochemical efficiency of 50%.

All experiments were analyzed using Zview software v.2.7 from Scribner Associates Inc.

3. Experimental results

3.1. Characteristics of M1, M2 and M3 magnesium samples

Tables 1 and 3 show the measured parameters of M1, M2 and M3 magnesium samples used in this study. Table 1 shows the difference in the measured values of electric charge per unit of mass loss (A h lb^{-1}), for each sample. These values were obtained using the ASTM [1] and NMX [2] methodology.

Table 2 shows the chemical composition of each sample, obtained by atomic absorption. It also includes the reference values indicated by the ASTM B 843 standard [4] for a high potential magnesium alloy. The chemical composition of the M1 sample falls within the required chemical composition range. M2 sample does not fulfill with the required content of Mg (98.3 wt.%), therefore does not match the expected chemical composition. Sample M3 does not fulfill the required chemical composition.

3.2. Open circuit potential against time (E_{oc} versus t)

Fig. 1(a) and (b) shows that, during all the exposure time, M3 sample shows the more noble values of E_{oc} ; M1 sample shows the more active values of E_{oc} ; while M2 sample shows values of E_{oc} between those of M1 and M3 values. These values are shown in Table 3. The measured data indicates that the M1 sample is the only one that fulfills the value of open circuit potential stated in the NMX standard [2].

3.3. Polarization curves

Measurement of the polarization behavior is a powerful method for determining the corrosion behavior of a metal over a wide range of oxidizing conditions in a single test solution. By varying the potential of the electrode, different oxidation conditions at the electrode surface can be examined. The corresponding current provides a measure of the

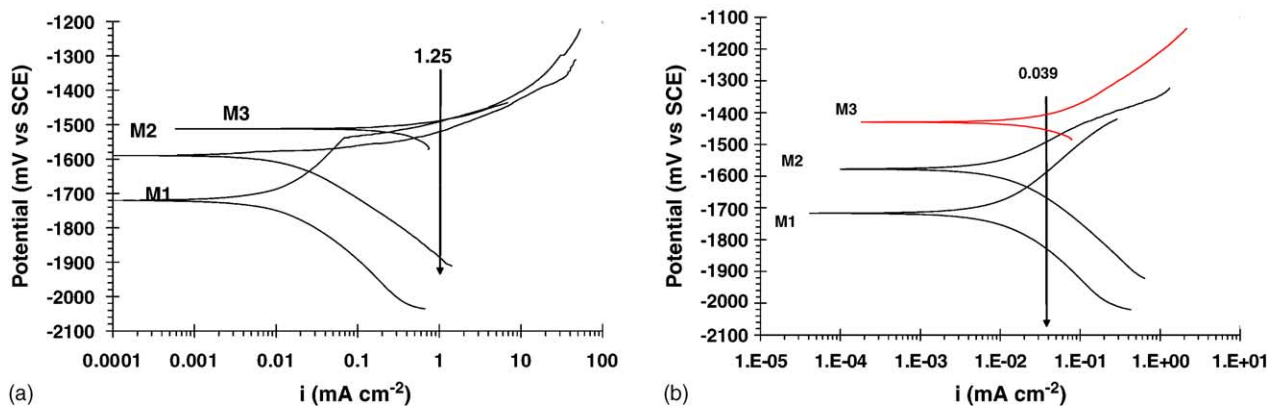


Fig. 1. (a and b) Polarization curves for M1, M2 and M3 magnesium alloy samples; (a) 3% NaCl solution (b) $\text{CaSO}_4 \cdot 2\text{H}_2\text{O} - \text{Mg}(\text{OH})_2$ solution (ASTM G 97-97), after 2.5 h of immersion time.

Table 4
Kinetic parameters calculated from polarization curves, from Fig. 1a and b

| Sample | i_{corr} (mA cm ⁻²) | | Tafel slope (mV) | | E_{corr} (mV vs. SCE) | |
|--------|--|-------------|------------------|-------------|--------------------------------|-------------|
| | 3% NaCl | ASTM G97-97 | 3% NaCl | ASTM G97-97 | 3% NaCl | ASTM G97-97 |
| M1 | 0.013 | 0.0079 | 253.2 | 199.4 | -1719.9 | -1719.8 |
| M2 | 0.358 | 0.0072 | 116.3 | 120.1 | -1590.2 | -1577.9 |
| M3 | 0.59 | 0.046 | 81.2 | 159.0 | -1513.0 | -1429.6 |

rate of the reactions at each potential. Potentiodynamic polarization techniques permit the measurement of polarization behavior by continuously scanning the potential while monitoring the current response. Polarization behavior is very helpful in determining Tafel regions, presence of passivity and regions where electrolyte resistivity can be a problem.

Fig. 1a and b shows the polarization curves, obtained in the two test solutions, for M1, M2 and M3 magnesium alloy samples. It is clear that the shape of the polarization curves is different for each sample in each environment. This difference can be associated to the different chemical composition of the magnesium alloy samples. Table 4 shows the kinetic parameters, estimated from the polarization curves. These parameters indicate that, at the E_{corr} , the 3% NaCl solution is more aggressive to the magnesium alloy samples, than the ASTM solution.

In Fig. 1a a current density value of 1.25 mA cm⁻² has been marked. This value corresponds to the current density indicated by the NMX test procedure [2], for the measurement of the electrical charge per unit of mass loss. In Fig. 1b a current density value of 0.039 mA cm⁻² has been marked. This value corresponds to the current density indicated by the ASTM test procedure [1] for the measurement of the electrical charge per unit of mass loss. Table 5 lists the anodic potential values for each sample, corresponding to the testing current density values, indicated by the NMX and ASTM procedures. These anodic potentials were directly read from the anodic branches of the polarization curves shown in Fig. 1a and b. These potentials correspond to values at which, each magnesium alloy sample, should be polarized when it is evaluated by the NMX or the ASTM method.

Table 5
Anodic potentials read on the measured polarization curves (Fig. 1a and b) for M1, M2 and M3 magnesium alloy samples, at the testing current densities, indicated by the NMX and ASTM methods

| Test solution | Sample | Anodic potential read on the polarization curve (mV vs. SCE) | |
|---------------|--------|--|-----------------------------|
| | | At 0.039 mA cm ⁻² | At 1.25 mA cm ⁻² |
| 3% NaCl | M1 | - | 240 |
| | M2 | - | 80 |
| | M3 | - | 30 |
| ASTM G97 | M1 | 120 | - |
| | M2 | 80 | - |
| | M3 | 20 | - |

Table 5 indicates that, at a constant testing anodic current density, each magnesium alloy sample will acquire a different anodic potential. In both testing solutions, the M3 sample is the one that is less polarized from its E_{oc} value. On the other hand, the M1 sample is the one that is more polarized from its E_{oc} value, in both testing solutions. It is important to note from Fig. 1a that the anodic branch of the polarization curve of M1 sample, exhibits a high value of Tafel slope of 253.2 mV, suggesting a passivation process taking place on the surface of the electrode. In this situation, a testing anodic current density value of 1.25 mA cm⁻² falls on a region of an activation controlled process of transpassivity.

3.4. Electrochemical Impedance spectroscopy (EIS) results

3.4.1. EIS behavior of M1 magnesium alloy sample in 3% NaCl solution at (E_{oc})

Fig. 2a and d shows the EIS data, measured at the E_{oc} , on sample M1 immersed in 3% NaCl solution after 6 h of immersion time. In the Nyquist plot two semicircles can be observed, with some degree of depression. The Bode representation confirms the presence of two time constants that can be associated to two parallel resistor–capacitor circuits. In order to analyze the experimental data an equivalent electrical circuit is proposed. This equivalent circuit considers the presence of a film of corrosion products upon the surface of the sample and a charge transfer process. In order to compensate the depression of the semicircle, observed in the Nyquist representation, a constant phase element was considered in the equivalent circuit. The equivalent circuit and the estimated values for each electric component are shown in Fig. 3 and presented in Figs. 6 and 7. Fig. 2a and d shows the good correlation between the experimental data and the data obtained in a simulation using the equivalent circuit proposed.

3.4.2. EIS behavior of M2 magnesium alloy sample in 3% NaCl solution at the open circuit potential (E_{oc})

The Nyquist representation, Fig. 2b, does not show the two semicircles found in Fig. 2a. However, in the Bode representation of the phase angle, two time constants can be detected, Fig. 2e. In this case, it was found that the behavior of the measured EIS values can be described with, essentially, the same

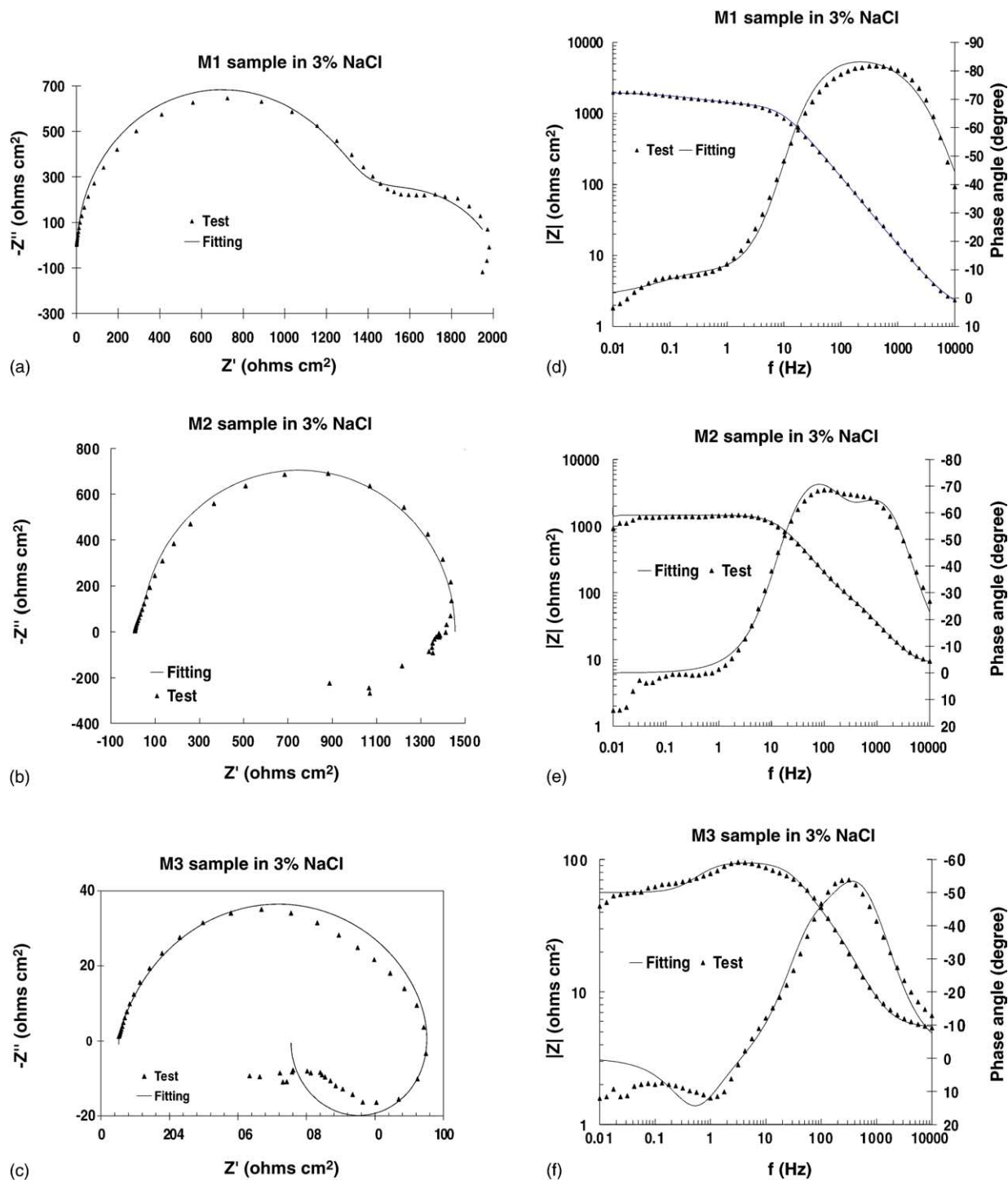


Fig. 2. (a–f) EIS spectra, Nyquists (a–c) and Bode (d–f) representations, at 6 h immersion time. Magnesium samples in 3% NaCl solution at the open circuit potential (E_{oc}).

equivalent circuit used in the analysis of the M1 sample. Two capacitors are considered in the equivalent circuit and the analyses shown that the constant phase element, used in the circuit in Fig. 3 was not necessary to obtain a good correlation between the measured data and the numerical simulation. Figs. 6 and 7 list the corresponding results for the equivalent circuit analysis.

3.4.3. EIS behavior of M3 magnesium alloy sample in 3% NaCl solution at the open circuit potential (E_{oc})

The Nyquist representation of the impedance, Fig. 2c shows a loop at lower frequencies. This feature has been associated to the presence of an inductor in an electrical equivalent circuit. This inductor has been associated to adsorption and desorption phenomena occurring on the surface of the sam-

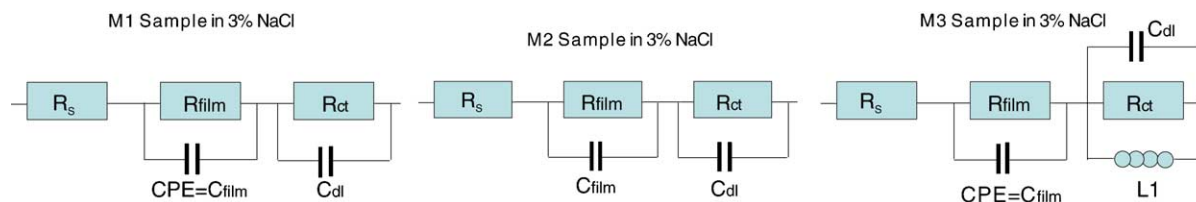


Fig. 3. Equivalent circuits, 3% NaCl solution.

ple [5–9]. The Bode representation of the impedance does not show a clear sharp maximum (see Fig. 2f), therefore, the presence of two time constants (associated to two capacitors) was assumed. Fig. 3 shows the electrical equivalent circuit that best fitted the measured data and the calculated values for each component in Figs. 6 and 7.

3.4.4. EIS behavior of M1 magnesium alloy sample in ASTM G97, solution at the open circuit potential (E_{oc})

The Nyquist representation of the impedance, Fig. 4a shows the presence of two semicircles, that can be associated to two resistor–capacitor circuits. This observation is confirmed in the Bode representation of the phase angle (Fig. 4d). Fig. 5 shows the electrical equivalent circuit that best fitted the measured impedance data and the corresponding values for each component are in Figs. 6 and 7. It was found that the use of a constant phase element (CPE) was needed in order to account for the depression of the semicircles [5,6,8]. However, the calculated values of the parameter n of the CPE, indicates that this component cannot be regarded as a pure capacitor [10].

3.4.5. EIS behavior of M2 magnesium alloy sample in ASTM G97, solution at the open circuit potential (E_{oc})

The Nyquist representation of the impedance, Fig. 4b shows two clear semicircles that can be associated to two time constants, therefore to two capacitors. This feature can also be observed in the Bode representation of the phase angle (Fig. 4e). As the mathematical analyses shown, the equivalent circuit in Fig. 5 can represent the measured impedance data. The corresponding calculated numerical values are shown in Figs. 6 and 7.

3.4.6. EIS behavior of M3 magnesium alloy sample in ASTM G97, solution at the open circuit potential (E_{oc})

The Nyquist representation of the impedance shows a loop at lower frequencies (Fig. 4c). This feature suggests that an inductor could be considered in the corresponding equivalent circuit. It was found that the electrical circuit shown in Fig. 5 can describe the measured impedance data. The calculated values of the electrical components in the circuit are presented in Figs. 6 and 7. A constant phase element was considered in the electrical equivalent circuit in order to account for the depression of the semicircles. Figs. 6–8 compare the calculated values for each component of the equivalent circuits that were shown in Figs. 3 and 5.

Fig. 6 shows that in general, the calculated values for the charge transfer resistance (R_{ct}) are higher in the ASTM solution than those values calculated in the 3% NaCl solution. This behavior will lead to a higher corrosion rate in the 3% NaCl solution, Fig. 8. This same trend is observed in the calculated values of the film resistance (R_{film}), indicating that the electrical properties of the film formed in either solution are different.

Corrosion and electrochemical behavior of magnesium samples were significantly influenced by chloride ions. The increase in corrosion rate in the 3% NaCl solution may be attributed to the participation of chloride ions in the dissolution reaction. Chloride ions are aggressive for magnesium. The adsorption of chloride ions to oxide covered magnesium surface transforms $Mg(OH)_2$ to easily soluble $MgCl_2$. In agreement with the above observations, the polarization curves, Fig. 1a and b exhibited an increase in anodic current density in NaCl solution, Fig. 1a as compared with $CaSO_4$ – $Mg(OH)_2$ solution, Fig. 1b.

Fig. 7 is a comparison of the calculated values of the capacitance associated to the surface film of corrosion products (C_{film}). It is found that the sample M3 has the highest C_{film} values. Considering that, C_{film} is inversely proportional to the thickness of the film formed on the surface of the electrode [11], it is possible to conclude that, in general, the M3 sample has the thinnest film formed on its surface [12]. Fig. 8 compares the calculated values of corrosion current density (i_{corr}) for samples M1, M2 and M3 [13]. A value of 0.026 V for the Stern–Geary constant was used in all calculations [14]. It is clear from this figure that the highest value of i_{corr} was determined on the surface of sample M3.

3.4.7. EIS behavior of the M1 magnesium alloy sample in 3% NaCl solution, polarized condition

In order to study the electrochemical behavior of the magnesium alloy samples in polarized conditions, EIS spectra were measured at three anodic potentials, selected on the polarization curve of sample M1, immersed in 3% NaCl solution. M1 anode sample was selected because was the only that fulfills with the chemical composition and electrochemical efficiency specified by the NMX standard. The selected overpotentials were: 85, 145 and 200 mV, away from E_{oc} . The polarization curve in Fig. 9 shows the location of the three selected over potentials.

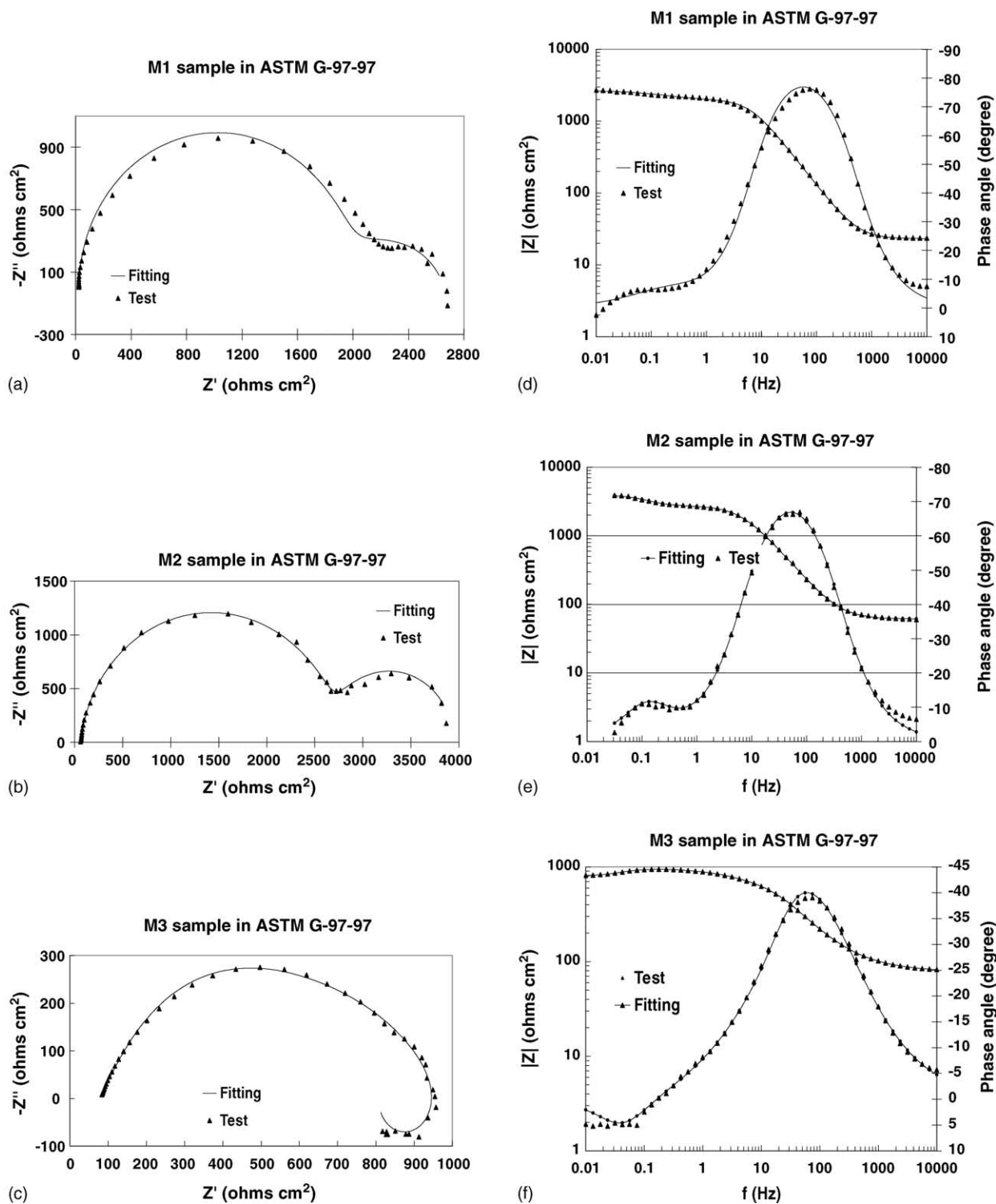


Fig. 4. (a–f) EIS spectra, Nyquists (a–c) and Bode (d–f) representations, at 6 h immersion time. Magnesium samples in ASTM G97 test solution at the open circuit potential (E_{oc}).

3.4.8. EIS behavior of M1 magnesium alloy sample in 3% NaCl solution, polarized condition, 85 mV of overpotential

It was found that the electrical equivalent circuit, showed in Fig. 11 can describe the measured impedance data at an

anodic overpotential of 0.85 mV, away from E_{oc} . This is illustrated in Fig. 10a and d. Figs. 12 and 13 show the estimated values of the electric components of the corresponding circuit. It can be seen that the estimated values of R_{film} and R_{ct} decrease as the overpotential increases.

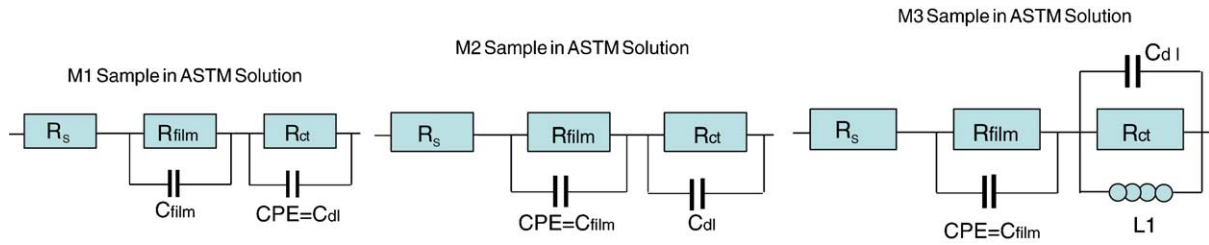


Fig. 5. Equivalent circuits, ASTM solution.

3.4.9. EIS behavior of the M1 magnesium alloy sample in 3% NaCl solution, polarized condition, 145 mV of overpotential

The Nyquist representation of the measured impedance shows a loop and a scattered data behavior at lower frequencies (Fig. 10b and e). This loop can be associated to an inductor in the corresponding electrical equivalent circuit. The Bode representation of the associated phase angle indicates the presence of two time constants, related to two capacitors–resistor circuits. It was found that the electrical

equivalent circuit shown in Fig. 11 can describe the measured impedance data obtained at 145 mV of overpotential. This is demonstrated in Fig. 10b and e. Figs. 12 and 13 present the estimated values for each component in the circuit in graphic form.

3.4.10. EIS behavior of M1 magnesium alloy sample in 3% NaCl solution, polarized condition, 200 mV of overpotential

The Nyquist representation of the measured impedance (Fig. 10c) shows a depressed semicircle. Also, a loop at lower frequencies can be detected. It is possible that this loop is

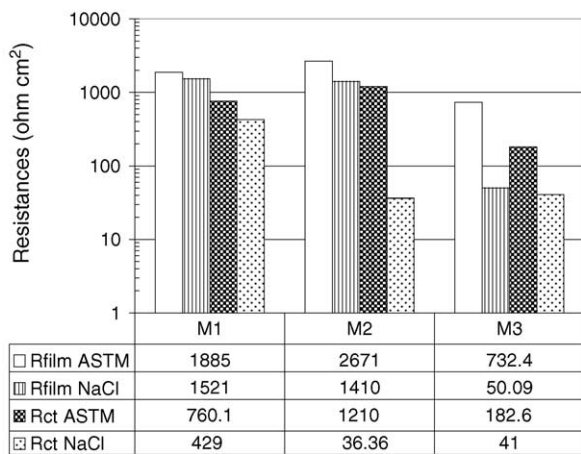


Fig. 6. Film resistances (R_{film}) and charge transfer resistances (R_{ct}), calculated for samples M1, M2 and M3, immersed in each testing solution. Data obtained from.

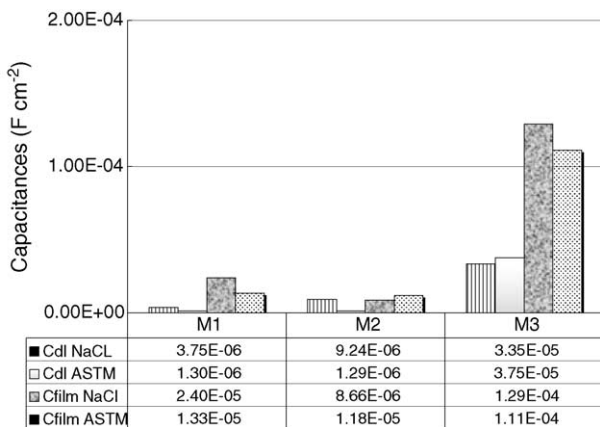


Fig. 7. Averaged values of double layer (C_{dl}) and film capacitances (C_{film}), calculated for samples M1, M2 and M3, immersed in each testing solution.

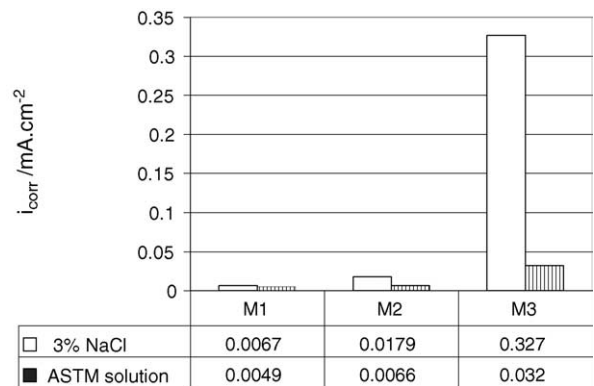


Fig. 8. Averaged values of corrosion current density (i_{corr}), calculated for samples M1, M2 and M3, immersed in each testing solution.

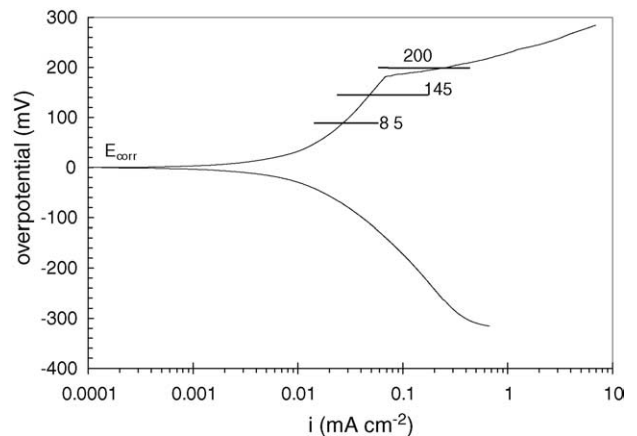


Fig. 9. Polarization curve for magnesium alloy sample M1 in 3% NaCl solution. Selected values of over potentials are indicated, where EIS data was obtained.

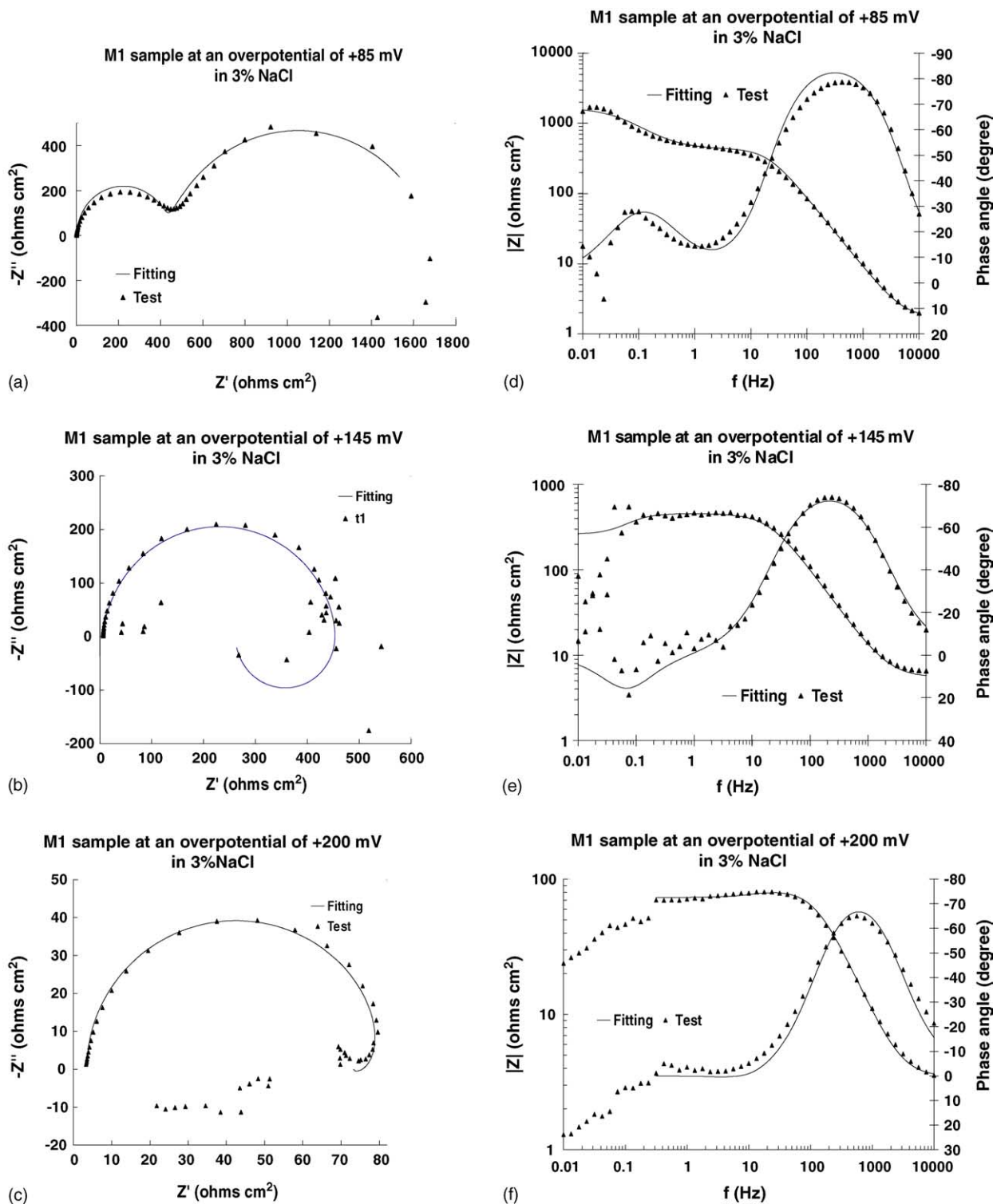


Fig. 10. (a–f) EIS spectra, Nyquist (a–c) and Bode (d–f) representations, at 6 h of immersion time. Magnesium samples in 3% NaCl solution. Polarized condition; 85, 145 and 200 mV of anodic overpotential.

associated to the formation, adsorption and desorption [5,9] of the corrosion products, on the surface of the electrode, as a consequence of the anodic polarization. In the Bode representation of the measured phase angle of the impedance (Fig. 10f), it is possible to identify two-time constants. The

shape of the Bode plots of the measured impedance also suggests the presence of two capacitor–resistor circuits, in the corresponding equivalent circuit. According to these observations, it was found that the equivalent circuit in Fig. 11 can describe the measured impedance data. Figs. 12 and 13

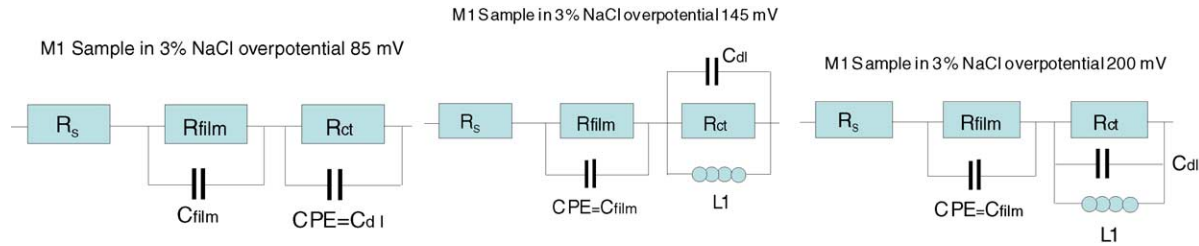


Fig. 11. Equivalent circuits 3% NaCl solution. Anodic overpotential of 85, 145 and 200 mV.

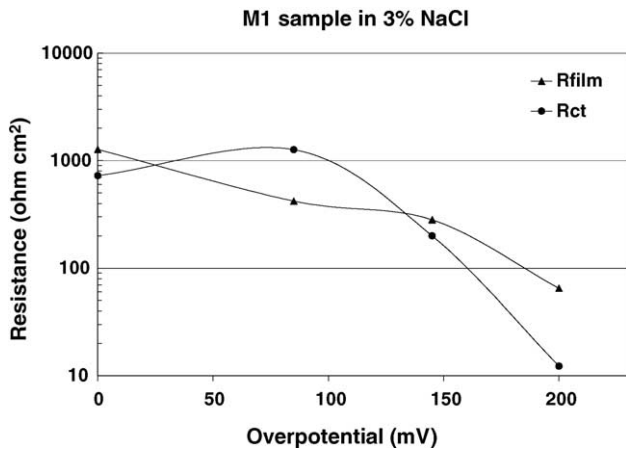


Fig. 12. Calculated resistances, associated to the film of corrosion products on the surface of the electrode (R_{film}) and to the charge transfer process occurring on the surface of the electrode (R_{ct}) as a function of the overpotential.

show the calculated values for each electric component of the equivalent circuit in Fig. 11.

Figs. 12 and 13 compare the calculated parameters of the resistance associated to the corrosion products film (R_{film}), as a function of the overpotential. In these figures it is possible to observe that, as the overpotential increases the calculated R_{film} decreases. This behavior is independent of the immersion time and the variation is about 1.5 orders of magnitude.

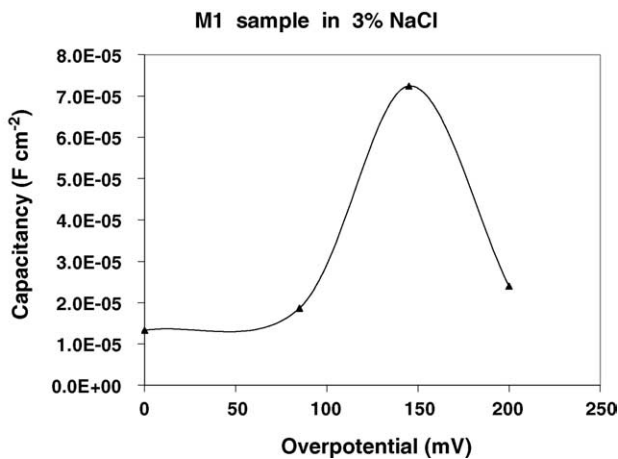


Fig. 13. Calculated capacitance associated to the film of corrosion products formed on the surface of the electrode (C_{film}) as a function of the overpotential.

Fig. 12 shows the behavior of the calculated charge transfer resistance (R_{ct}), associated to the electrochemical processes occurring on the surface of the metal, as a function of the polarization of the electrode. As it is expected, R_{ct} decreases as the polarization increases. This behavior is a direct consequence of the increment in the dissolution rate of the magnesium alloy, due to the polarization of the sample. Fig. 13 shows the measured values of the capacitance associated to the film of corrosion products (C_{film}), as a function of the overpotential. It was found that, at 145 mV of overpotential, C_{film} reaches a maximum value.

These observations give clear idea of how the polarization of the electrode influences the electrochemical process taking place on the surface of the metal and the formation of the film of corrosion products [15].

3.5. X-ray diffraction analysis

A sample of the solids formed on the surface of the M1 magnesium alloy electrode was taken and analyzed by X-ray diffraction. This was done in order to identify the chemical compounds in the layer of corrosion products. These analyses indicated that the corrosion products formed, in both testing solutions, were magnesium hydroxide [11,16].

4. Conclusions

The results presented in this work lead to the following conclusions:

1. The chemical composition influences the electrochemical behavior of each magnesium alloy sample, defining the parameters: open circuit potential (E_{oc}), corrosion current density (i_{corr}), cathodic and anodic slopes. This fact leads to consider that, when an anodic current is applied to a sample, in order to measure the corresponding mass loss, each alloy will acquire a different potential, defined in the polarization curve. Therefore, each alloy will not be evaluated at the same anodic condition.
2. The corrosion process of a magnesium alloy, intended to work as a sacrificial anode for cathodic protection systems, and evaluated in laboratory in either a 3% NaCl solution or the testing solution indicated in the ASTM G97 procedure, can be described by a simple electrical equivalent circuit made of: one resistor, associated

- to the solution resistance (R_s), in series with two parallel resistor–capacitor (R – C) circuits, both connected in series. One circuit representing the charge transfer process taking place on the surface of the alloy R_{ct} – C_{dl} and a second circuit associated to the film of corrosion products formed on the surface of the electrode R_{film} – C_{film} .
3. When a magnesium alloy does not fulfill the chemical composition specified for a sacrificial magnesium anode, features as inductive loops appear in the Nyquist representation of the measured impedance. This fact leads to consider the presence of inductors in the corresponding electrical equivalent circuit.
 4. It was found that, when a magnesium alloy, intended to work as a sacrificial anode, is polarized at a constant anodic potential, near the open circuit potential (E_{oc}), the dissolution process can be described by an electrical equivalent circuit similar to the one described in 2.
 5. As the magnesium alloy is polarized farther away from its E_{oc} , in the anodic direction, the Nyquist representation of the impedance exhibits inductive loop behavior. This fact leads to consider an inductor component in the corresponding electrical equivalent circuit. This inductive loop can be associated to the process of formation of the corrosion products layer on the surface of the electrode.
 6. The main corrosion product formed on the surface of the magnesium alloy samples, immersed in either, 3% NaCl solution or ASTM G97 testing solution, was identified as magnesium hydroxide.

References

- [1] Standard Test Method for Laboratory Evaluation of Magnesium Sacrificial Anode Test Specimens for Underground Applications. ASTM G 97-97, Philadelphia, p. 1, 1997.
- [2] Mexican Standard NMX-K-109-1977, “Anodos de Magnesio Empleados en Protección Catódica”, General Direction of Standards, Mexico D.F., 11 November 1997 (Approved and published).
- [3] H.A. Robinson, P.F. George, *Corrosion* 10 (1954) 182.
- [4] Standard Specification for Magnesium Alloy Anodes for Cathodic Protection, ASTM B 843-98, Philadelphia, 1998.
- [5] J.G. Kim, S.J. Koo, *Corrosion* 56 (4) (2000) 380.
- [6] R. Cottis, S. Turgoose, Electrochemical impedance and noise, in: C.S. Barry (Ed.), *Testing Made Easy*, NACE International, Houston, 1999.
- [7] J.H. Greenblatt, *J. Electrochem. Soc.* 103 (10) (1956) 539.
- [8] T. Pajkossy, *J. Electroanal. Chem.* 364 (1994) 111.
- [9] W.M. Chan, F.T. Cheng, L.K. Leung, R.J. Horylev, T.M. Yue., *Corrosion* 97, Paper No. 441, NACE International, Houston, 1997.
- [10] C.H. Hsu, Mansfeld, *Corrosion* 57 (9) (2001) 747.
- [11] J. Genesca, L. Betancourt, C. Rodriguez, *Corrosion* 52 (7) (1996) 502.
- [12] N. Pebere, C. Riera, F. Dabosi, *Electrochim. Acta* 35 (2) (1990) 555.
- [13] Standard Practice for calculation of corrosion rates and related information from electrochemical measurements ASTM G102-89 (Reapproved 1999).
- [14] D.D. MacDonald, *J. Electrochem. Soc.* 12 (1978) 2062.
- [15] G. Song, A. Atrens, D. St Johns, X. Wu, J. Nairn, *Corros. Sci.* 39 (10–11) (1997) 1981.
- [16] G.R. Hoey, M. Cohen, *J. Electrochem. Soc.* 105 (5) (1958) 245.